

# Bandwidth Allocation for Cloud-Augmented Autonomous Driving

Peter Schafhalter\*  
Sylvia Ratnasamy

Alexander Krentsel\*  
Scott Shenker  
UC Berkeley ICSI

Joseph E. Gonzalez  
Ion Stoica

## Abstract

Autonomous vehicle (AV) control systems increasingly rely on ML models for tasks such as perception and planning. Current practice is to run these models on the car’s local hardware due to real-time latency constraints and reliability concerns, which limits model size and thus accuracy. Prior work has observed that we could augment current systems by running larger models in the cloud, relying on faster cloud runtimes to offset the cellular network latency. However, prior work does not account for an important practical constraint: limited cellular bandwidth. We show that, for typical bandwidth levels, proposed techniques for cloud-augmented AV models take too long to transfer data, thus mostly falling back to the on-car models and resulting in no accuracy improvement.

In this work, we show that realizing cloud-augmented AV models requires intelligent use of this scarce bandwidth, i.e. carefully allocating bandwidth across tasks and providing multiple data compression and model options. We formulate this as a resource allocation problem to maximize car utility, and present our system *TURBO* which achieves an increase in average model accuracy by up to 15 percentage points on driving scenarios from the Waymo Open Dataset.

## 1. Introduction

Breakthroughs in ML model architectures, infrastructure, and training techniques over the past decade have produced models that far surpass heuristic-based systems for autonomous vehicles (AVs) [21, 67, 81, 99, 114]. Although these advances have led to a handful of real-world deployments [3, 17], improving model accuracy remains a key goal as deployments continue to experience challenges due to the long tail of possible scenarios such as operation in poor weather conditions and construction zones [19, 20, 27].

One solution to improve accuracy is to use larger, more capable models [88, 97, 121]. However, scaling models on-vehicle poses key challenges: (i) models with more FLOPs

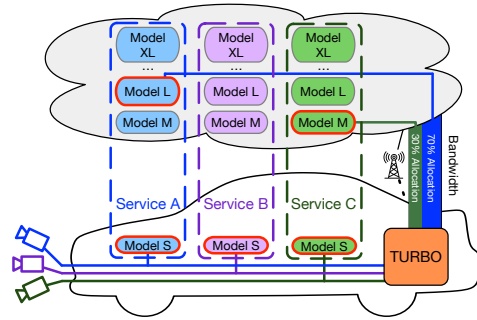


Figure 1: *TURBO* offers larger and more accurate cloud models to the on-car control system, optimally selecting the subset of inputs to send and models to run in the cloud and apportioning bandwidth.

have larger inference runtimes, whereas AVs require rapid response times to ensure safety, (ii) on-vehicle hardware is limited compared to a data center due to physical constraints on power, cooling, and vehicle stability, and (iii) the high cost of state-of-the-art ML accelerators is economically incompatible with vehicle pricing. For these reasons, the computer chips deployed on-vehicle are an order of magnitude<sup>1</sup> less powerful than the hardware available in datacenters. Considering that AVs must operate with faster-than-human reaction times (e.g. 0.39 to 1.2 s [59, 113]), the deployment of models on-vehicle requires a careful navigation of the tradeoffs between runtime and accuracy to ensure both high-quality decision-making and rapid response times [40, 48, 104].

Recent works [28, 95] propose leveraging low-latency 5G networks to augment AVs with cloud compute, by opportunistically executing highly accurate, large models in the cloud while continuing to run small models on-vehicle. The AV uses the highly accurate results from the cloud as long as they arrive in time; otherwise, the AV falls back to the results from the on-vehicle model, thus improving accuracy with no risk of degrading reliability. However, these works do not consider the crucial issue of bandwidth: AVs generate over 8 Gbps of data across different sensing modalities<sup>2</sup> [51, 107] used as inputs to the control system, far exceeding the 250

<sup>1</sup>A single SOTA cloud GPU (H100) can perform over 10× more operations per second than AV-targeted chips like NVIDIA’s DRIVE Orin [4, 6].

<sup>2</sup>A 10 Hz camera generating 1920×1280 frames contributes 590 Mbps.

\*Equal contribution

Mbps target uplink bandwidth for 5G networks [57]. The bandwidth-induced overhead alone to transfer this volume of data far exceeds runtime service-level objectives (SLOs, or deadlines). We observe that while these data volumes make it infeasible to move the entire control system to the cloud, it is feasible to transmit a limited *subset* of the input data to enable certain control system models to receive their input and return their results within SLO. However, two key questions arise: what subset of inputs to send, and how much bandwidth to allocate to each of them.

In this work, we introduce our system, TURBO – Task Utility and Resource Bandwidth Optimizer – which manages optimal model selection and bandwidth allocation across input data streams as network conditions change. Our approach builds on the observation that different control system tasks have different bandwidth requirements and experience widely varying benefits from access to additional compute. For example, a front camera feed with many distant objects derives more benefit from a highly accurate object detector running in the cloud than a side camera feed with few, close-by objects. Intuitively, allocating more bandwidth to a task reduces its network latency, enabling within-SLO execution of slower and more accurate models; as bandwidth is scarce, allocating to one service necessarily prevents other services from running in the cloud.

Recognizing the intrinsic tie between cloud model selection and bandwidth allocation, we formulate an optimization problem that solves these jointly. As we discuss in more detail in §3, we encode the relationship between bandwidth allocation, model selection, and task accuracy for each task as *bandwidth-accuracy utility curves* [25, 110]. Our system then combines these into a global bandwidth allocation optimization problem, solving for and enforcing per-task input bandwidth allocations as network conditions change to maximize cumulative benefit to the car. To further improve performance across variable network conditions, our system seamlessly supports multiple cloud model variants of varying input size, runtime, and accuracy, greedily selecting the best possible configuration for each task, all while continuing to run on-vehicle models in parallel as a fallback.

We show that operating with SOTA open-source models (§4) on the Waymo Open Dataset [102], our system improves *average* accuracy by up to 15.6 percentage points (pp) over executing on-vehicle only and 12.7 pp over naive bandwidth allocation methods (§5). We conclude with a discussion of the implications of our work and future directions (§6).

## 2. Related Work

**Runtime-accuracy tradeoffs.** AVs rely on highly accurate models to perceive their surroundings, predict the future, and plan safe trajectories. This pipeline of models must execute quickly to outperform human reaction times of 390ms to 1.2s [59, 113]. Recent AV systems [48, 49] provide on-

vehicle model selection to respond to dynamic service SLOs by optimizing tradeoffs in runtime and accuracy. Our work is complementary, augmenting these on-vehicle models with larger cloud models selected considering their SLOs and available network bandwidth. Existing approaches to video analytics [22, 37, 58, 60, 69, 76, 116, 117, 122] aim to provide high accuracy on real-time metrics [68, 96] while addressing tradeoffs in runtime and network utilization. However, these do not address cross-service contention for bandwidth, which is core to our problem and method.

**Scalable Model Architectures.** Recent advances in model architectures enable the development of more accurate models by increasing the number of parameters [77, 97, 108, 121]. To address the increased computational requirements of larger models, researchers often develop model *families* which provide different tradeoff points between resource requirements and accuracy as shown in Fig. 10 using EfficientDet [104] for perception. The same is possible for state-of-the-art motion prediction models leveraging transformers [85, 98]. We leverage these model families to balance latency, input size, and accuracy, selecting among multiple configurations to adapt to changing network conditions.

**Role of the Network in Autonomous Driving.** AVs occasionally rely on cellular networks for remote interventions, in which an AV contacts a remote human operator for guidance [80, 106]. Prior works propose decentralized systems that build on Vehicle-to-Vehicle or Vehicle-to-Infrastructure communication to harness additional compute resources [33, 75, 101, 103], share data [65, 89, 125], or develop collaborative algorithms [30, 73, 86, 109]. While such approaches and edge-cloud model partitioning methods [61, 90, 124] improve the accuracy of individual AV services, our work addresses the key problem of holistically partitioning bandwidth across all services while operating in fluctuating network conditions. Prior works in networking consider utility-based bandwidth allocation for centralized traffic engineering in data centers and WANs [25, 41, 55, 64, 74, 82]; we formulate a utility curve composition in a *client* with dynamic cloud model options, optimizing bandwidth across services within a single application.

## 3. Method

The AV control system today consists of multiple *services*, such as object detection for each camera, which process inputs (e.g., camera frames) and produce outputs (e.g., bounding boxes). Each service is subject to a *service-level objective* (SLO) that defines its maximum runtime, and the highest accuracy available model that satisfies this SLO on the car’s compute is chosen at design time to run on-car.

Our method (Fig. 1) augments this system by allowing a subset of services to additionally run in the cloud, allocating bandwidth to transmit their inputs based on the current network conditions. The on-car models run regardless in case

no response is received by the SLO. We offer each service an additional  $N$  cloud-based model options, each with its own input size, runtime, and (increased) accuracy. The decisions of which to use are non-trivial and dynamic; intuitively, for some amount of bandwidth, it may be best to have two services run on a medium cloud model, but slightly more bandwidth may unlock sending inputs in time for just one large model with greater cumulative benefit to the car.

To guide these decisions, we extend the concept of “utility curves” [25] to quantify a service’s accuracy given a bandwidth allocation. We show in the following sections how at system design time we derive service-level utility curves from the cloud-model configurations (§3.1, §3.2) to capture bandwidth-accuracy tradeoffs, then how at runtime, we solve an Integer Linear Program (ILP) formulation that allocates bandwidth and selects cloud models to maximize overall application-wide utility (§3.3).

### 3.1. Model-Level Utility

A model’s utility must capture both the model’s performance (*i.e.* accuracy) as well as whether it completes within its SLOs (*i.e.* latency), as a function of allocated bandwidth. For a model  $m$  with accuracy  $A$ , latency SLO  $t_{SLO}$ , and total runtime  $T_{rt}(b, t_{RTT})$  (where  $b$  is allocated bandwidth and  $t_{RTT}$  is the round-trip time), the utility is:

$$U_m(b) = \begin{cases} A_m & T(b, t_{RTT}) \leq t_{SLO} \\ 0 & T(b, t_{RTT}) > t_{SLO} \end{cases} \quad (1)$$

$U_m(b)$  is a unit step function where utility is 0 when the SLO is violated, and utility equals the model’s accuracy when the SLO is met. Because on-vehicle models are configured to meet latency SLOs and are unaffected by network transfer times, utility curves of on-vehicle are constant:

$$U_{\text{on-vehicle model}}(b) = A_{\text{on-vehicle model}} \quad (2)$$

In contrast, the runtime of models executing on remote resources depends on the allocated bandwidth, the characteristics of the model, and the network conditions. Given model input size  $S_{\text{input}}$ , round trip time  $t_{RTT}$ , and execution time  $t_{\text{exec}}$ , the total runtime of the model is:

$$T_{\text{remote model}}(b, t_{RTT}) = t_{\text{exec}} + t_{RTT} + \frac{S_{\text{input}}}{b} \quad (3)$$

This produces the following utility curve which is a step function from 0 to  $A$  where the step occurs at  $b_c$  when  $T(b_c, t_{RTT}) = t_{SLO}$ :

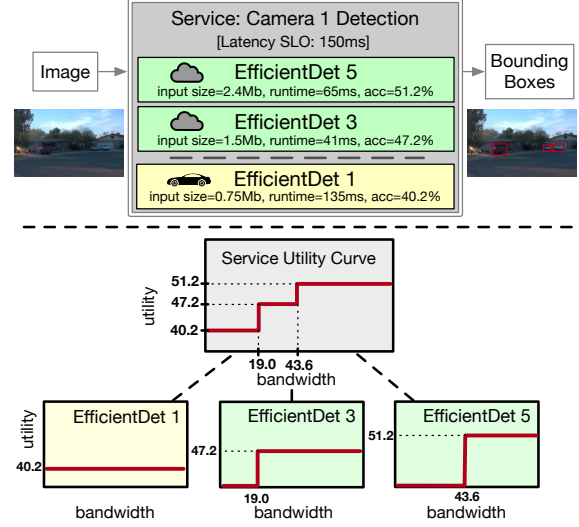


Figure 2: Utility curves for a service with 3 obj. detection models.

$$U_{\text{remote model}}(b) = \begin{cases} A_{\text{remote model}} & t_{\text{exec}} + t_{RTT} + \frac{S_{\text{input}}}{b} \leq t_{SLO} \\ 0 & \text{otherwise} \end{cases} \quad (4)$$

$$b_c = \frac{S_{\text{input}}}{t_{SLO} - t_{\text{exec}} - t_{RTT}} \quad (5)$$

A key consequence of the step-utility function is that  $b_c$  is the minimal bandwidth to run a remote model which is optimal when bandwidth is scarce. Bandwidth allocations greater than  $b_c$  provide the same utility of  $A_m$  as a bandwidth allocation of exactly  $b_c$ . Thus, excess bandwidth is wasted. Moreover, any bandwidth allocation less than  $b_c$  has a utility of 0, so bandwidth allocations  $0 < b < b_c$  are also wasted.

We also observe that more accurate models typically have larger inputs  $S_{\text{input}}$  and longer execution times  $t_{\text{exec}}$ . Consequently, more accurate models typically require larger bandwidth allocations  $b$  and are less tolerant of large round trip times  $t_{RTT}$  compared to their less accurate counterparts.

### 3.2. Service-Level Utility

A *service* represents a specific task, such as obstacle detection on a camera stream, and includes multiple models with varying parameters and resource requirements. The service runs the best feasible model on-vehicle, while additional models can execute in the cloud.

To handle disconnections and bandwidth fluctuations, the on-vehicle model always runs as a fallback [95]. This ensures that **the service always provides a minimum utility of  $A_{\text{local model}}$** , making remote execution a *strict improvement* over local-only operation.

We define the utility function of a service  $s$  as the control-application utility, *i.e.* accuracy, gained from allocating it bandwidth  $b$ . The service should always choose the model

that results in the highest utility given the bandwidth, therefore service utility is the maximum utility over models  $\mathcal{M}$ :

$$U_s(b) = \max_{m \in \mathcal{M}} U_m(b) \quad (6)$$

Fig. 2 illustrates a service-level utility curve for object detection, where a small EfficientDet D1 (ED1) model runs on the car, while larger ED3 and ED5 models are available in the cloud. Since higher-accuracy models require more bandwidth to satisfy SLOs,  $U_s(b)$  forms a step function, with steps occurring when bandwidth allows a transition to a more accurate model. The optimal allocation is the selected model's bandwidth requirement  $b_c$ , or 0 if running locally; any other allocation would waste bandwidth. Each service runs at most one remote model<sup>3</sup>. Thus, bandwidth allocation effectively determines which model (if any) runs remotely.

### 3.3. Runtime Bandwidth Allocation

At runtime, our goal is to determine which subset of input data to transfer to cloud-models, and at what data-rate, in order to maximize "utility" to the car. This allocation must change in response to varying network conditions (bandwidth, RTT), which we can measure using standard methods [39, 42]. In order to do this, we propose a general framework for formulating application level utility from all utilities of all services:

$$U_{\text{app}}(b) = \max_{b_s: s \in \mathcal{S}} \sum_{s \in \mathcal{S}} f_s(U_s(b_s)) : \sum_{b_s: s \in \mathcal{S}} b_s \leq b \quad (7)$$

Our formulation exposes a *transformation function*  $f_s: \mathbb{R} \rightarrow \mathbb{R}$  that allows an operator flexibility to re-weight each service's relative priorities based on their contribution to an operator-chosen goal.  $f_s$  can be arbitrary, *i.e.* linear to prioritize more important services, sigmoid to normalize utility values to a common scale, or the identity function to maximize total accuracy across all services. Because  $U_s(b)$  is a step function,  $f_s \circ U_s$  is piecewise linear and defined by  $f_s(U_s(b_{c,s,m}))$  where  $b_{c,s,m}$  is the bandwidth at which the steps occur for each model  $m$  from the set of models the service has access to  $\mathcal{M}_s$ , ensuring a linear objective.

We then frame bandwidth allocation as a utility maximization problem over this application utility (Eq. (7)), considering available bandwidth and RTT. Our approach formulates this as an Integer Linear Program (ILP); the step-function nature of service utility functions allows the ILP to directly select optimal cloud model configurations. Let  $\mathcal{S}$  be the set of services and  $\mathcal{M}_s$  be the set of models available to service  $s$ . The utility function of service  $s$  is a step function defined by the accuracies  $a_m$  of each model  $m \in \mathcal{M}_s$  with the steps located at the critical bandwidths  $b_{c,m}$ .

<sup>3</sup>Running multiple cloud models and selecting results before the SLO is possible but computationally expensive; we do not explore this design.

We define binary decision variables:

$$x_{m,s} = \begin{cases} 1 & \text{if model } m \text{ of service } s \text{ is selected,} \\ 0 & \text{otherwise.} \end{cases} \quad (8)$$

**Objective Function:** Maximize the total utility across all services. For simplicity, we use  $f_s(x) = x$ , but this can be tuned to prioritize key services.

$$\max_x \sum_{s \in \mathcal{S}} \sum_{m \in \mathcal{M}_s} x_{s,m} \cdot a_{s,m} \quad (9)$$

**Constraints:**

*Bandwidth Constraint:* The total allocated bandwidth across all services must not exceed the available bandwidth:

$$\sum_{s \in \mathcal{S}} \sum_{m \in \mathcal{M}_s} x_{s,m} \cdot b_{c,s,m} \leq B \quad (10)$$

*One Cloud Model per Service Constraint:* Each service must be allocated one model configuration:

$$\sum_{m \in \mathcal{M}_s} x_{s,m} = 1 \quad \text{for each } s \in \mathcal{S} \quad (11)$$

*Binary Constraint:* The decision variables are binary, reflecting the discrete nature of the utility allocation:

$$y_{m,s} \in \{0, 1\} \quad \text{for all } m \in \mathcal{M}_s, s \in \mathcal{S} \quad (12)$$

This ILP formulation directly selects which models configurations to run for the cloud across a set of services while maximizing the overall utility to the application. As a result, the ILP solution also produces the optimal bandwidth allocations for each service, based on each selected model's  $b_c$ . In §4, we apply this method to derive utility functions using state-of-the-art models, and evaluate its ability to boost the accuracy of autonomous driving services in §5.

## 4. Design and Implementation

### 4.1. Resource Model

We model the AV as a resource-constrained edge device with an NVIDIA Jetson Orin, the same chip in the NVIDIA DRIVE Orin platform [10], which powers autonomous driving for Volvo and SAIC [66]. The AV is assumed to have sufficient compute to run a pipelined AV software stack with resource-efficient ML models that meet accuracy and runtime SLOs. The cloud, in contrast, is a resource-rich environment capable of processing incoming data with more accurate ML models. We assume cloud models execute on an NVIDIA H100 GPU via a RunPod 1×H100 PCIe instance with 176 GB RAM and 16 vCPUs.

Existing ML serving systems optimize efficiency through batching and economies of scale [32, 50, 93]. These approaches complement our work by enhancing resource utilization and reducing deployment costs.

Model	Input [Mb]	Preprocessing [ms]		Inference [ms]	
		Orin	H100	Orin	H100
ED1	9.8	18	11	118	21
ED2	14.2	20	12	166	23
ED4	25.2	25	15	523	30
ED6	39.3	37	18	1350	54
ED7x	56.6	43	25	2320	91

Table 1: *EfficientDet* models. Preprocessing measures the runtime of resizing and preparing the image on CPU. Inference includes transferring pre-processed data to GPU and running the model.

## 4.2. Tasks

### 4.2.1. Object Detection

We first examine object detection, a representative computer vision task, and its potential benefits from cloud computing. Object detection is well-studied, with numerous open-source models [23, 26, 92, 104] and datasets [34, 45, 72, 102, 118], and shares design patterns (e.g., CNNs) with other perception tasks like semantic segmentation and 3D object detection. Our object detection SLO is 150 ms,

**Models.** We study the EfficientDet family of models [104] because they provide a large trade-off space across accuracy, latency, and resource requirements which we benchmark in Tab. 1. We use EfficientDet-D1 (ED1) as the on-vehicle model, as it is the most accurate model that meets the SLO within local compute constraints. Cloud models include ED2, ED4, ED6, and ED7x, which provide increasing accuracy but exceed the SLO when run on-vehicle.

EfficientDet models perform lightweight on-CPU preprocessing to resize images before deep neural network (DNN) inference on the GPU. We leverage this preprocessing and various compression strategies to define multiple inference configurations, each offering different trade-offs between runtime, accuracy, and data transfer overhead (Fig. 3):

1. *Cloud preprocessing* offloads both image preprocessing and inference to the cloud, minimizing on-device computation but requiring the largest data transfer.
2. *On-vehicle preprocessing* preprocesses images locally to transfer less data to the cloud, reducing bandwidth usage at the cost of local processing overhead.
3. *Image compression* applies lossless PNG or lossy JPEG compression to the raw image before transfer, decreasing data size but introducing (de)compression delays.
4. *DNN input compression* compresses preprocessed model inputs before transfer, achieving the highest reduction in data size while incurring largest runtime overhead.

**Dataset.** We train and evaluate detection models using the Waymo Open Dataset (WOD) v2.0.0 [102], which contains 6.4 hours of driving data across 1,150 scenes of 20 seconds sampled at 10 Hz, annotated with 9.9 million bounding boxes. WOD provides five camera perspectives, each treated as a distinct task. The front, front-left, and front-right cameras capture images at a resolution of  $1920 \times 1280$ , while the

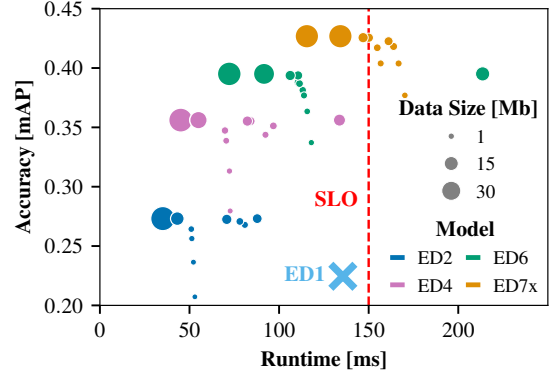


Figure 3: We consider 35 model configurations with different tradeoffs in runtime, accuracy, and data transfer size: ED1 runs on-vehicle while ED2, ED4, ED6, and ED7x execute in the cloud. We generate additional configurations by applying lossless PNG and lossy JPEG compression to either the original image or the pre-processed model inputs. Our JPEG quality factors are 95, 90, 75, and 50. We find that compression significantly reduces the amount of data to transfer at the cost of increased runtime and reduced accuracy.

side cameras capture  $1920 \times 886$ , resulting in uncompressed image sizes of 59 Mb and 41 Mb, respectively. At P99, images contain 62 ground truth bounding boxes, yielding an output size of 7.9 Kb.<sup>4</sup>

**Training.** We partition the scenes from the WOD v2.0.0 [102] into training (68%), validation (12%), and test (20%) sets. To match the dataset, we modify the models to recognize five classes of objects: vehicles, pedestrians, cyclists, signs, and other. We initialized the models with pre-trained weights from the COCO dataset [72] provided by [112], and fine-tune on the WOD dataset for 10 epochs<sup>5</sup>.

### 4.3. Motion Prediction

Motion prediction is a key autonomous driving task that estimates the future positions of nearby agents (e.g. vehicles, pedestrians, cyclists). It is an active area of research exploring various neural network architectures. We set an SLO of 250 ms based on reported runtimes of open-source AV implementations [1, 49]. While models use both high-definition (HD) maps and historical agent trajectories as inputs, we transmit only agent information, as maps can be precomputed and stored in the cloud.

**Models.** For cloud-based prediction, we use Motion Transformer [98], a state-of-the-art model employing a Transformer architecture, ranked first on the 2022 Waymo Open Motion Dataset [40] (WOMD) leaderboard. For on-vehicle predictions, we select MotionCNN [62], a lightweight model

<sup>4</sup>Each bounding box consists of four 32-bit floating point numbers for the minimum and maximum x and y coordinates, along with an 8-bit integer for the class.

<sup>5</sup>We fine-tune ED7x for only 8 epochs due to the high cost of training. Note our system performance would be strictly better if trained 10 epochs.

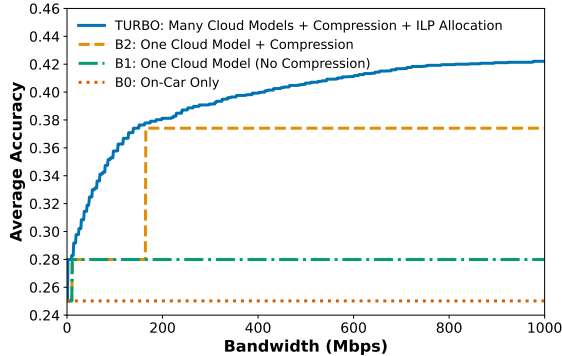


Figure 4: Average accuracy across services for TURBO compared to baselines of varying naivete as bandwidth increases. We assume an RTT of 20ms, object detection SLOs of 150ms, and motion planning SLO of 250ms, averaging performance across all scenarios.

that ranked third on the 2021 WOMD leaderboard. MotionCNN represents trajectories and surroundings as a fixed-resolution image and uses a convolutional neural network to predict future paths.

**Dataset.** We train and evaluate models using WOMD v1.2.1, which contains over 100k scenes of 20 seconds sampled at 10 Hz, split into training (70%), validation (15%), and test (15%) sets. WOMD includes 3D bounding boxes for each agent and scene map data (e.g. lanes, signs, crosswalks). Models predict agent positions at three, five, and eight seconds into the future using an HD map and a one-second trajectory history. The cloud-based Motion Transformer model has a P99 input size of 146 Kb and a P99 output size of 246 Kb.

**Training.** We modify the open-source implementations of Motion Transformer and MotionCNN for compatibility with WOMD v1.2.1, and follow the published training procedures. Our trained models achieve validation accuracies of 0.22 mAP for MotionCNN and 0.40 for Motion Transformer.

#### 4.4. Utility Functions

We follow Sec. 3.1 to construct utility functions for each model configuration, using SLOs of 150 ms for object detection and 250 ms for motion prediction. Cloud models are profiled with the Jetson Orin for preprocessing and compression and the H100 for preprocessing, inference, and postprocessing. We compute  $t_{\text{exec}}$  using P99 values and measure the data transfer per inference iteration, setting  $S_{\text{input}}$  to its P99 value. While the raw images and preprocessed EfficientDet inputs have large but fixed data sizes, compression takes additional time to execute and results in variable but smaller data sizes (Fig. 3). Similarly, the Motion Transformer’s input size depends on the number of agents in the scene, so we estimate the input size as the P99 value. Using these profiles, we apply Eq. (5) to determine the bandwidth threshold  $b_c$  at which each model can complete within SLO.

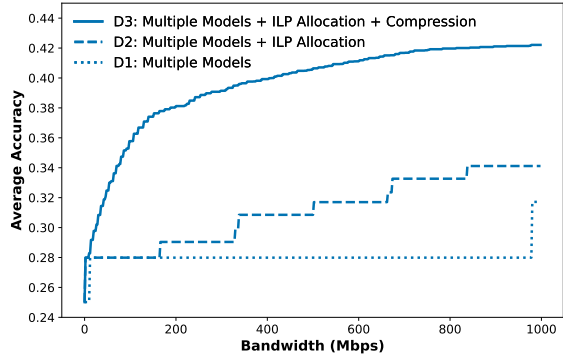


Figure 5: Incremental benefit from TURBO’s design decisions.

To compute service-level utility, we incorporate all cloud models along with the on-vehicle model, which serves as a performance floor as it always runs. We weight all services equally, setting  $f_s(u) = u$  in our optimization objective.

#### 4.5. ILP Implementation

We model our ILP in Python using PuLP [94] using the measured accuracy, runtime, and data transfer requirements measured in Sec. 4.2 in conjunction with the RTT and available bandwidth. We use the CBC solver [44] to solve the ILP which selects the cloud model configurations for the object detection and motion planning services. Because AVs consist of tens of services with access to tens of models each, the optimization space is small, so our solver operates in real time. Experimentally, we measure a solver runtime of 27-32 ms with an unoptimized Python implementation.

### 5. Evaluation

In this section, we analyze the benefit in accuracy our AV receives from using TURBO and how this accuracy is impacted by the specific design choices we make.

**Quantifying AV Benefit.** The ultimate goal of AV control system development is maintaining and improving AV safety, which is measured by the frequency of “disengagements” [87] and the frequency of crashes [13, 105]. To this end, one may evaluate AV behavior in a simulator [48] and measure occurrence of incidents. However this necessitates using synthetic environment data as input.

We opt for using real-world production data in our evaluation, as the real-world images enable us to use and evaluate real detection models. While this prevents us from reporting a decreased “crash rate” number as we cannot modify the action that the car takes in the pre-recorded scenario, we are instead able to quantify exactly how much service accuracy increases on real-world sensor data, which leads directly to improved environment perception and thus more faithful planning. We provide an example in which a better model detects a mid-distance pedestrian that the on-vehicle model misses in Fig. 10 of Appendix A.

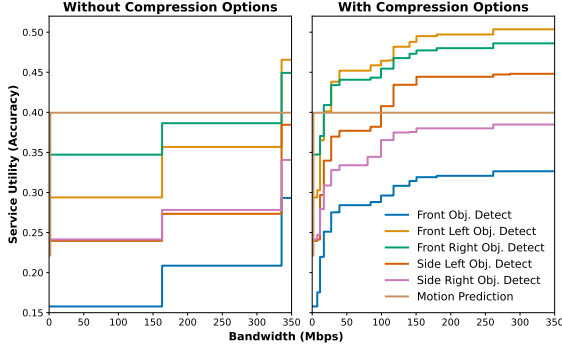


Figure 6: Utility curves for each service as derived by TURBO, without (left) and with (right) compression options considered, showing each service’s accuracy if allocated  $x$  units of bandwidth.

**Setup.** We conduct our evaluation on the Waymo Open Dataset [102] described in Sec. 4.2, for the six competing services reported in the same section; five detection services running for each of the five camera views provided in the dataset, and the motion prediction service.<sup>6</sup> We evaluate on-car and cloud performance on the hardware reported in Sec. 4.1, measuring the pre-processing, compression, decompression, and model runtime for each model configuration on both the car and cloud hardware, to construct end-to-end runtimes of each selected configuration across car and cloud.

**TURBO Accuracy vs. Baselines.** Fig. 4 compares our method to three baseline tiers (B) under varying network bandwidth, with RTT fixed at 20ms (per [83] for a server within 500km). B0 runs only on-car models, using the highest-accuracy model that runs within SLO (ED1 for object detection, a CNN for motion planning). B1 adds a single cloud model option per service (ED4 for object detection, a transformer for motion planning), sharing bandwidth equally as is the default behavior across datastreams on a network [31]. B2 preprocesses and compresses object detection inputs (ED4 with on-car preprocessing, JPEG at 90% quality) before network transfer, but still shares bandwidth equally (i.e. without utility-aware bandwidth allocation).

TURBO (solid blue) improves on baselines by up to 15.6 pp by being bandwidth- and utility-aware, enabling optimal bandwidth allocation, and adaptive preprocessing and compression based on available bandwidth. In B1, after an initial bump from the motion planning service moving to the cloud, camera services see no benefit until well over 2Gbps (not shown), as without special attention to bandwidth allocation as we propose, the network enforces equal bandwidth across datastreams by default via TCP [31]. B2 shifts this

<sup>6</sup>Motion planning depends on results of object detection; in this work, we assume pipelined execution of the AV control program [2, 48, 107], thus bundle motion planning using the results of earlier perception along with perception on newly collected data. While it is conceivable to optimize further by moving multiple sequential dependencies to the cloud to avoid round-trips to the car, it is out of scope for our work; we leave such an investigation to future work.

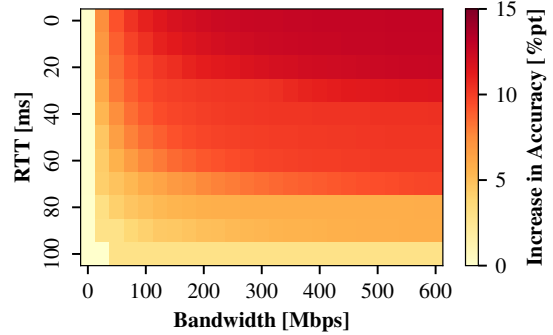


Figure 7: Average percentage point accuracy gain on the WOD across all services for various network conditions.

step earlier but still provides only a single transition point. In contrast, TURBO dynamically prioritizes services with the highest accuracy gains – allocating bandwidth early to motion planning (leftmost jump in the graph per Sec. 4.3) – and continues adjusting allocations to maximize accuracy.

**Factor Analysis** TURBO achieves its performance through three key design ideas: (D1) selecting from multiple models based on bandwidth, (D2) optimizing selection via a utility-maximizing ILP, and (D3) dynamically applying compression. Fig. 5 shows their relative contributions. Our gains stem from their synergy. Multiple cloud model options enable earlier upgrades (at 980Mbps in Fig. 5), but default equal bandwidth sharing forces all upgrades to happen at once. ILP-based allocation prioritizes allows more bandwidth to services that benefit more from upgrading the model they run. Finally, compression unlocks more opportunities at lower bandwidths, expanding ILP optimization points (Fig. 6).

**Varying Network Conditions** TURBO provides variable benefit based on the network conditions available. Fig. 7 shows the mean increase in accuracy across all scenarios for a range of bandwidth and RTT network conditions. While higher bandwidth and lower latency always provides more benefit, we see up to 10 pp higher accuracy with as little as 150Mbps with RTTs of 20ms, well within the experienced operating ranges provided by 5G [47, 57, 83].

## 5.1. Dynamic Utility Curves

In our analysis, we find that model accuracy varies significantly across frames and services (Fig. 9 in appendix). Intuitively, this can be influenced by environmental factors, e.g. wet roads increase reflections in the front cameras and side cameras capture less light at night. Thus, we also explore the benefit of *dynamic* utility curves per environment or frame group, evaluating four policies with varying “freshness”:

1. **Global Static:** static utility curves derived from average accuracy across all frames of all scenarios, used above.
2. **Scenario Static:** utility curves static to each scenario in the dataset, derived from the average accuracy across all

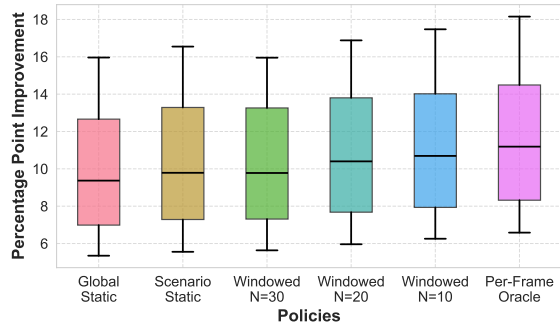


Figure 8: The distribution of percentage point improvement over on-car-only models for each utility curve policy, ranging from most static on the left to most dynamic on the right, assuming 250Mbps of bandwidth and 20ms RTT. 5, 25, 50, 75, 95th percentiles shown.

frames of the particular scenario.

3. **N-Windowed**: utility curve computed from the  $N^{\text{th}}$  frame of each scenario, used for the next  $N - 1$  frames. We experiment with  $N = 10, 20, 30, 50$ .
4. **Per-Frame Oracle**: optimal ground-truth utility curve for each frame for each scenario, using the actual accuracy of each model on that frame.

Fig. 8 shows accuracy improvements over on-car-only models. The Per-Frame Oracle sets an upper bound, achieving a +11.30 pp median improvement over on-vehicle models and +1.84 pp over global static.

Recomputing utility curves for new accuracy values on each frame is impractical. A more feasible approach, the windowed  $N=20$  policy, yields a 10.51 pp median improvement over on-vehicle models and +1.05 pp over global static. This suggests that dynamically adjusting utility provides a small but meaningful accuracy boost, enabling AVs to optimize bandwidth allocation based on environmental conditions.

**Accurate estimation of ground truth.** While the “global static” curve can be derived from extensive past data, dynamic curves require estimating model accuracy per environment and window *at runtime* – an open problem [96] beyond this work’s scope. However, determining the relative accuracy differences between models could be sufficient. One potential approach is to periodically upload high-resolution images using spare bandwidth to run all models, and estimate relative accuracy by comparing outputs to the predictions generated by the largest state-of-the-art “golden” model. We leave the evaluation of such strategies to future work.

## 6. Discussion

**Network reliability.** Though cellular connectivity is widespread, particularly in urban areas [5, 11] targeted for AV deployment, variance in network performance remains a challenge [115]. TURBO always runs on-car models to ensure safety in case of network degradation, and periodically reallocates bandwidth to maximize accuracy gain. However, highly variable network conditions can lead to either under-

utilization of bandwidth or missed SLOs, both resulting in less-than-optimal accuracy gain. To mitigate network variance, operators can tune the network measurement module to use more conservative estimates of network conditions (i.e., leave ‘buffer room’ in the latency budget). Additionally, operators can integrate recent works which show high accuracy in making short-term 5G bandwidth and latency predictions [79, 119, 123].

**Cost.** Successful large-scale deployments are sensitive to economic feasibility of a system. In Appendix A.1, we estimate our total hourly cost of remote resources at \$5.27, with \$2.78 from the network (at the 10th global percentile) and \$2.49 from compute for an H100. We emphasize that the true cost of cloud compute is likely lower due to better efficiency when operating at scale. Our method is tunable for cost-sensitive markets: operators can tune their utility curves to take into account cost-benefit, *e.g.* by executing on cheaper GPUs and selectively using cloud models in challenging environments.

**End-to-end models for AVs.** As an alternative to service-based approaches, end-to-end models [54, 56, 70, 120] directly predict actions from sensor data, enabling the joint optimization of all driving tasks. TURBO benefits end-to-end models by enabling the cloud execution of higher quality sub-networks (*e.g.* encoders for a sensor modality), which can improve driving performance by scaling up models to larger parameter counts when network conditions allow.

**Applications beyond AVs.** We believe that the benefits of using cloud hardware in real-time to boost accuracy has far-reaching applications. Beyond AVs, TURBO can benefit vehicles with limited autonomy, such as hands-free highway driving or self-parking. Similarly, autonomous drones use ML to process sensor data in real time. Drones exhibit even more stringent constraints on compute due to weight restrictions, making access to cloud resources an attractive option. Robotics [29], security systems, and vision-language models are other applications which benefit from real-time access to cloud resources to benefit accuracy.

We discuss a number of additional implications from this work in Appendix A.3.

## 7. Conclusion

Cloud computing enables AVs to run highly accurate and computationally intensive ML models by shifting resource limitations from the compute that can be deployed on-vehicle to network bandwidth. Because the amount of data AVs produce far exceeds the capabilities of 5G networks, AVs must carefully prioritize what data to upload to maximize the benefit (*i.e.* safety) to the overall system. To address these issues, we introduce TURBO which augments AV services with models running in the cloud by optimizing tradeoffs in accuracy, runtime, and data transmission size. Our solution maximizes accuracy across all services using the available bandwidth and scales with



different network conditions. We believe that TURBO is an important step towards addressing the hardware limitations of AVs, and provides a general foundation for building data-intensive networked AI applications.

## References

- [1] Apollo. <https://github.com/ApolloAuto/apollo/>. Accessed: 2024-9-5. 5
- [2] Autoware concepts. <https://autowarefoundation.github.io/autoware-documentation/galactic/design/autoware-concepts/>. Accessed 2024-9-18. 7
- [3] Cruise to launch robotaxi services in austin, phoenix before end of 2022. <https://techcrunch.com/2022/09/12/cruise-to-launch-robotaxi-services-in-austin-phoenix-before-end-of-2022/>. 1, 15
- [4] Drive agx orin developer kit. <https://developer.nvidia.com/drive/agx>. Accessed 2024-6-11. 1
- [5] Mobile LTE coverage map. <https://www.fcc.gov/BroadbandData/MobileMaps/mobile-map>. Accessed: 2025-2-23. 8
- [6] Nvidia h100 tensor core gpu. <https://www.nvidia.com/en-us/data-center/h100/>. Accessed 2024-6-11. 1
- [7] Delivery robots for everyone! <https://www.kiwibot.com/>. Accessed: 2024-9-18. 16
- [8] Gpu cloud. <https://lambdalabs.com/service/gpu-cloud>. Accessed 2024-6-23. 15
- [9] What is quantum computing. <https://azure.microsoft.com/en-us/resources/cloud-computing-dictionary/what-is-quantum-computing>. Accessed: 2024-9-19. 16
- [10] Nvidia drive developer faq. <https://developer.nvidia.com/drive/faq>. Accessed 2024-6-23. 4
- [11] 5G & 4G LTE coverage map: Check your cell phone service. <https://www.t-mobile.com/coverage/coverage-map>. Accessed: 2025-2-23. 8
- [12] Next stop for waymo one: Los angeles. <https://waymo.com/blog/2022/10/next-stop-for-waymo-one-los-angeles.html>. 15
- [13] Waymo safety impact. <https://waymo.com/safety/impact/>. Accessed 2024-9-18. 6, 15
- [14] Zoox. <https://zoox.com/>. Accessed: 2024-9-18. 16
- [15] Network coverage forecast – ericsson mobility report. <https://www.ericsson.com/en/reports-and-papers/mobility-report/dataforecasts/network-coverage>, 2020. Accessed: 2024-9-19. 16
- [16] *Honda News*, 2023. 16
- [17] Scaling waymo one safely across four cities this year. <https://waymo.com/blog/2024/03/scaling-waymo-one-safely-across-four-cities-this-year/>, 2024. 1, 15
- [18] Federal Highway Administration. Table mv-1 - highway statistics 2022. <https://www.fhwa.dot.gov/policyinformation/statistics/2022/mv1.cfm>, 2023. 16
- [19] National Highway Traffic Safety Administration. Collision between vehicle controlled by developmental automated driving system and pedestrian. <https://www.nts.gov/investigations/accidentreports/reports/har1903.pdf>, 2018. 1
- [20] National Highway Traffic Safety Administration. Part 573 safety recall report 23e-086, 2023. 1
- [21] Mayank Bansal, Alex Krizhevsky, and Abhijit Ogale. Chauffeurnet: Learning to drive by imitating the best and synthesizing the worst. *arXiv preprint arXiv:1812.03079*, 2018. 1
- [22] Romil Bhardwaj, Zhengxu Xia, Ganesh Ananthanarayanan, Junchen Jiang, Yuanhao Shu, Nikolaos Karianakis, Kevin Hsieh, Paramvir Bahl, and Ion Stoica. Ekya: Continuous learning of video analytics models on edge compute servers. In *19th USENIX Symposium on Networked Systems Design and Implementation (NSDI 22)*, pages 119–135, 2022. 2
- [23] Alexey Bochkovskiy, Chien-Yao Wang, and Hong-Yuan Mark Liao. YOLOv4: Optimal speed and accuracy of object detection. 2020. 5
- [24] Bureau of Transportation Statistics. Average age of automobiles and trucks in operation in the united states, 2024. 16
- [25] Zhiruo Cao and E W Zegura. Utility max-min: an application-oriented bandwidth allocation scheme. In *IEEE INFOCOM '99. Conference on Computer Communications. Proceedings. Eighteenth Annual Joint Conference of the IEEE Computer and Communications Societies. The Future is Now (Cat. No.99CH36320)*, pages 793–801 vol.2. IEEE, 1999. 2, 3
- [26] Nicolas Carion, Francisco Massa, Gabriel Synnaeve, Nicolas Usunier, Alexander Kirillov, and Sergey Zagoruyko. End-to-end object detection with transformers. In *Computer Vision—ECCV 2020: 16th European Conference, Glasgow, UK, August 23–28, 2020, Proceedings, Part I 16*. Springer, 2020. 5
- [27] Max Chafkin. Even after \$100 billion, self-driving cars are going nowhere. <https://www.bloomberg.com/news/features/2022-10-06/even-after-100-billion-self-driving-cars-are-going-nowhere>, 2022. 1
- [28] Kaiyuan Chen, Nan Tian, Christian Juette, Tianshuang Qiu, Liu Ren, John Kubiawicz, and Ken Goldberg. Fogros2-plr: Probabilistic latency-reliability for cloud robotics, 2024. 1
- [29] Kaiyuan Eric Chen, Yafei Liang, Nikhil Jha, Jeffrey Ichnowski, Michael Danielczuk, Joseph Gonzalez, John Kubiawicz, and Ken Goldberg. Fogros: An adaptive framework for automating fog robotics deployment. In *2021 IEEE 17th International Conference on Automation Science and Engineering (CASE)*, pages 2035–2042. IEEE, 2021. 8
- [30] Qi Chen, Xu Ma, Sihai Tang, Jingda Guo, Qing Yang, and Song Fu. F-cooper: Feature based cooperative perception for

- autonomous vehicle edge computing system using 3d point clouds. In *Proceedings of the 4th ACM/IEEE Symposium on Edge Computing*, pages 88–100, 2019. 2
- [31] Dah-Ming Chiu and Raj Jain. Analysis of the increase and decrease algorithms for congestion avoidance in computer networks. *Computer Networks and ISDN Systems*, 17(1): 1–14, 1989. 7
- [32] Daniel Crankshaw, Xin Wang, Guilio Zhou, Michael J Franklin, Joseph E Gonzalez, and Ion Stoica. Clipper: A Low-Latency Online Prediction Serving System. In *Proceedings of the 14<sup>th</sup> USENIX Conference on Networked Systems Design and Implementation (NSDI)*, pages 613–627, 2017. 4, 15
- [33] Mingyue Cui, Shipeng Zhong, Boyang Li, Xu Chen, and Kai Huang. Offloading autonomous driving services via edge computing. *IEEE Internet of Things Journal*, 7(10): 10535–10547, 2020. 2
- [34] Jia Deng, Wei Dong, Richard Socher, Li-Jia Li, Kai Li, and Li Fei-Fei. Imagenet: A large-scale hierarchical image database. In *2009 IEEE conference on computer vision and pattern recognition*, pages 248–255. Ieee, 2009. 5
- [35] Derek Chiao, Johannes Deichmann, Kersten Heineke, Ani Kelkar, Martin Kellner, Elizabeth Scarinci, Dmitry Tolstinev. Autonomous vehicles moving forward: Perspectives from industry leaders. Technical report, McKinsey, 2024. 15
- [36] Alexey Dosovitskiy, Lucas Beyer, Alexander Kolesnikov, Dirk Weissenborn, Xiaohua Zhai, Thomas Unterthiner, Mostafa Dehghani, Matthias Minderer, Georg Heigold, Sylvain Gelly, et al. An image is worth 16x16 words: Transformers for image recognition at scale. *arXiv preprint arXiv:2010.11929*, 2020. 16
- [37] Kuntai Du, Ahsan Pervaiz, Xin Yuan, Aakanksha Chowdhery, Qizheng Zhang, Henry Hoffmann, and Junchen Jiang. Server-driven video streaming for deep learning inference. In *Proceedings of the Annual conference of the ACM Special Interest Group on Data Communication on the applications, technologies, architectures, and protocols for computer communication*, pages 557–570, 2020. 2
- [38] Arndt Ellinghorst, Meike Becker, Neil Beveridge, Bob Brackett, Danielle Chigumira, Oswald Clint, Chad Dillard, Brian Foran, Venugopal Garre, Jay Huang, Cherry Leung, Mark Li, Zhihan Ma, A.M. (Toni) Sacconaghi, Jean Ann Salisbury, Deepa Venkateswaran, Lu Wang, Robert Wildhack, and Gunther Zechmann. Electric revolution 2021: From dream to scare to reality?, 2021. 17
- [39] ESnet. iperf3, 2024. 4
- [40] Scott Ettinger, Shuyang Cheng, Benjamin Caine, Chenxi Liu, Hang Zhao, Sabeek Pradhan, Yuning Chai, Ben Sapp, Charles R Qi, Yin Zhou, et al. Large scale interactive motion forecasting for autonomous driving: The waymo open motion dataset. In *Proceedings of the IEEE/CVF International Conference on Computer Vision*, pages 9710–9719, 2021. 1, 5
- [41] A K Maulloo F P Kelly and D K H Tan. Rate control for communication networks: shadow prices, proportional fairness and stability. *Journal of the Operational Research Society*, 49(3):237–252, 1998. 2
- [42] Bill Fink and Rob Scott. nuttcp. 4
- [43] FiveThirtyEight. Uber pickups in new york city. <https://www.kaggle.com/datasets/fivethirtyeight/uber-pickups-in-new-york-city>. Accessed 2024-6-23. 15
- [44] John Forrest, Ted Ralphs, Stefan Vigerske, Haroldo Gambini Santos, John Forrest, Lou Hafer, Bjarni Kristjansson, jpfasano, EdwinStraver, Jan-Willem, Miles Lubin, rlougee, a andre, jggoncal1, Samuel Brito, h-i gassmann, Cristina, Matthew Saltzman, tostost, Bruno Pitrus, Fumiaki MATSUSHIMA, Patrick Vossler, Ron @ SWGY, and to st. coin-or/cbc: Release releases/2.10.12, 2024. 6
- [45] Andreas Geiger, Philip Lenz, and Raquel Urtasun. Are we ready for Autonomous Driving? The KITTI Vision Benchmark Suite. In *Proceedings of the IEEE Conference on Computer Vision and Pattern Recognition (CVPR)*, 2012. 5
- [46] Andrea Gemmet and Malea Martin. Driverless food delivery: Nuro teams up with uber eats to deploy autonomous vehicles in mountain view. <https://www.paloaltoonline.com/news/2022/09/11/driverless-food-delivery-nuro-teams-up-with-uber-eats-to-deploy-autonomous-vehicles-in-mountain-view/>, 2022. 16
- [47] Moinak Ghoshal, Z Jonny Kong, Qiang Xu, Zixiao Lu, Shivan Aggarwal, Imran Khan, Yuanjie Li, Y Charlie Hu, and Dimitrios Koutsonikolas. An in-depth study of uplink performance of 5g mmwave networks. In *Proceedings of the ACM SIGCOMM Workshop on 5G and Beyond Network Measurements, Modeling, and Use Cases*, pages 29–35, 2022. 7
- [48] Ionel Gog, Sukrit Kalra, Peter Schafhalter, Matthew A. Wright, Joseph E. Gonzalez, and Ion Stoica. Pylot: A Modular Platform for Exploring Latency-Accuracy Tradeoffs in Autonomous Vehicles. In *Proceedings of the IEEE International Conference on Robotics and Automation (ICRA)*, pages 8806–8813. IEEE, 2021. 1, 2, 6, 7
- [49] Ionel Gog, Sukrit Kalra, Peter Schafhalter, Joseph E Gonzalez, and Ion Stoica. D3: A Dynamic Deadline-Driven approach for Building Autonomous Vehicles. In *Proceedings of the Seventeenth European Conference on Computer Systems*, pages 453–471, 2022. 2, 5
- [50] Arpan Gujarati, Reza Karimi, Safya Alzayat, Antoine Kaufmann, Ymir Vigfusson, and Jonathan Mace. Serving DNNs like Clockwork: Performance Predictability from the Bottom Up. In *Proceedings of the 14<sup>th</sup> USENIX Symposium on Operating Systems Design and Implementation (OSDI)*, 2020. 4, 15
- [51] Florian Götz. The data deluge: What do we do with the data generated by avs? <https://blogs.sw.siemens.com/polarion/the-data-deluge-what-do-we-do-with-the-data-generated-by-avs/>, 2021. 1
- [52] Ralph Heredia. How to Cost-Effectively manage IoT data plans. <https://www.zipitwireless.com/blog/how-to-cost-effectively-manage-iot-data-plans>, 2023. Accessed: 2024-6-15. 15
- [53] Dan Howdle. Worldwide mobile data pricing 2023. <https://www.cable.co.uk/mobiles/worldwide-data-pricing/>. Accessed: 2024-6-13. 15

- [54] Yihan Hu, Jiazhi Yang, Li Chen, Keyu Li, Chonghao Sima, Xizhou Zhu, Siqi Chai, Senyao Du, Tianwei Lin, Wenhai Wang, et al. Planning-oriented autonomous driving. In *Proceedings of the IEEE/CVF Conference on Computer Vision and Pattern Recognition*, pages 17853–17862, 2023. 8
- [55] Xiaohong Huang, Tingting Yuan, and Maode Ma. Utility-optimized flow-level bandwidth allocation in hybrid sdn. *IEEE Access*, 6:20279–20290, 2018. 2
- [56] Jyh-Jing Hwang, Runsheng Xu, Hubert Lin, Wei-Chih Hung, Jingwei Ji, Kristy Choi, Di Huang, Tong He, Paul Covington, Benjamin Sapp, Yin Zhou, James Guo, Dragomir Anguelov, and Mingxing Tan. Emma: End-to-end multimodal model for autonomous driving. *arXiv preprint arXiv:2410.23262*, 2024. 8
- [57] International Telecommunications Union. Report ITU-R m.2410-0: Minimum requirements related to technical performance for IMT-2020 radio interface(s). Technical Report M.2410-0, International Telecommunications Union, 2017. 2, 7
- [58] Junchen Jiang, Ganesh Ananthanarayanan, Peter Bodik, Siddhartha Sen, and Ion Stoica. Chameleon: Scalable Adaptation of Video Analytics. In *Proceedings of the ACM Special Interest Group on Data Communication Conference (SIGCOMM)*, pages 253–266, 2018. 2
- [59] Gunnar Johansson and Kåre Rumar. Drivers’ brake reaction times. *Human factors*, 13(1):23–27, 1971. 1, 2
- [60] Daniel Kang, John Emmons, Firas Abuzaid, Peter Bailis, and Matei Zaharia. Noscope: optimizing neural network queries over video at scale. page 1586–1597. VLDB Endowment, 2017. 2
- [61] Yiping Kang, Johann Hauswald, Cao Gao, Austin Rovinski, Trevor Mudge, Jason Mars, and Lingjia Tang. Neurosurgeon: Collaborative intelligence between the cloud and mobile edge. *ACM SIGARCH Computer Architecture News*, 45(1): 615–629, 2017. 2
- [62] Stepan Konev, Kirill Brodt, and Artsiom Sanakoyeu. Motioncnn: A strong baseline for motion prediction in autonomous driving. *arXiv preprint arXiv:2206.02163*, 2022. 5
- [63] KPMG. Self-driving cars: The next revolution. <https://institutes.kpmg.us/content/dam/institutes/en/manufacturing/pdfs/2017/self-driving-cars-next-revolution-new.pdf>. 15
- [64] Alok Kumar, Sushant Jain, Uday Naik, Anand Raghuraman, Nikhil Kasinadhuni, Enrique Cauich Zermeno, C Stephen Gunn, Jing Ai, Björn Carlin, Mihai Amaranandei-Stavila, Mathieu Robin, Aspi Siganporia, Stephen Stuart, and Amin Vahdat. BwE: Flexible, hierarchical bandwidth allocation for WAN distributed computing. In *Proceedings of the 2015 ACM Conference on Special Interest Group on Data Communication*, pages 1–14, New York, NY, USA, 2015. Association for Computing Machinery. 2
- [65] Swarun Kumar, Shyamnath Gollakota, and Dina Katabi. A cloud-assisted design for autonomous driving. In *Proceedings of the first edition of the MCC workshop on Mobile cloud computing*, pages 41–46, 2012. 2
- [66] Marie Labrie. Volvo cars, zoox, saic and more join growing range of autonomous vehicle makers using new nvidia drive solutions. <https://nvidianews.nvidia.com/news/volvo-cars-zoox-saic-and-more-join-growing-range-of-autonomous-vehicle-makers-using-new-nvidia-drive-solutions>, 2021. 4
- [67] Zhaoqi Leng, Pei Sun, Tong He, Dragomir Anguelov, and Mingxing Tan. Pvtransformer: Point-to-voxel transformer for scalable 3d object detection, 2024. 1
- [68] Mengtian Li, Yuxiong Wang, and Deva Ramanan. Towards Streaming Perception. In *Proceedings of the European Conference on Computer Vision (ECCV)*, 2020. 2
- [69] Yuanqi Li, Arthi Padmanabhan, Pengzhan Zhao, Yufei Wang, Guoqing Harry Xu, and Ravi Netravali. Reducto: On-camera filtering for resource-efficient real-time video analytics. In *Proceedings of the Annual conference of the ACM Special Interest Group on Data Communication on the applications, technologies, architectures, and protocols for computer communication*, pages 359–376, 2020. 2
- [70] Zhiqi Li, Zhiding Yu, Shiyi Lan, Jiahan Li, Jan Kautz, Tong Lu, and Jose M Alvarez. Is ego status all you need for open-loop end-to-end autonomous driving? In *Proceedings of the IEEE/CVF Conference on Computer Vision and Pattern Recognition*, pages 14864–14873, 2024. 8
- [71] Shih-Chieh Lin, Yunqi Zhang, Chang-Hong Hsu, Matt Skach, Md E. Haque, Lingjia Tang, and Jason Mars. The Architectural Implications of Autonomous Driving: Constraints and Acceleration. In *Proceedings of the 23<sup>rd</sup> International Conference on Architectural Support for Programming Languages and Operating Systems (ASPLOS)*, pages 751–766, 2018. 16
- [72] Tsung-Yi Lin, Michael Maire, Serge Belongie, James Hays, Pietro Perona, Deva Ramanan, Piotr Dollár, and C Lawrence Zitnick. Microsoft CoCo: Common Objects in Context. In *Proceedings of the European Conference on Computer Vision (ECCV)*, pages 740–755. Springer, 2014. 5
- [73] Bing Liu, Qing Shi, Zhuoyue Song, and Abdelkader El Kamel. Trajectory planning for autonomous intersection management of connected vehicles. *Simulation Modelling Practice and Theory*, 90:16–30, 2019. 2
- [74] Changbin Liu, Lei Shi, and Bin Liu. Utility-based bandwidth allocation for triple-play services. In *Fourth European Conference on Universal Multiservice Networks (ECUMN’07)*, pages 327–336, 2007. 2
- [75] Luyang Liu, Hongyu Li, and Marco Gruteser. Edge assisted real-time object detection for mobile augmented reality. In *The 25th annual international conference on mobile computing and networking*, pages 1–16, 2019. 2
- [76] Shaoshan Liu, Liangkai Liu, Jie Tang, Bo Yu, Yifan Wang, and Weisong Shi. Edge computing for autonomous driving: Opportunities and challenges. *Proceedings of the IEEE*, 107(8):1697–1716, 2019. 2
- [77] Ze Liu, Yutong Lin, Yue Cao, Han Hu, Yixuan Wei, Zheng Zhang, Stephen Lin, and Baining Guo. Swin transformer: Hierarchical vision transformer using shifted windows. In *Proceedings of the IEEE/CVF international conference on computer vision*, pages 10012–10022, 2021. 2

- [78] Zhuang Liu, Hanzi Mao, Chao-Yuan Wu, Christoph Feichtenhofer, Trevor Darrell, and Saining Xie. A convnet for the 2020s. In *Proceedings of the IEEE/CVF Conference on Computer Vision and Pattern Recognition*, pages 11976–11986, 2022. 16
- [79] Jiamei Lv, Yuxiang Lin, Mingxin Hou, Yeming Li, Yi Gao, and Wei Dong. Accurate bandwidth and delay prediction for 5G cellular networks. *ACM Trans. Internet Technol.*, 2025. 8
- [80] Cade Metz, Jason Henry, Ben Laffin, Rebecca Lieberman, and Yiwen Lu. How self-driving cars get help from humans hundreds of miles away. *The New York Times*, 2024. 2
- [81] Norman Mu, Jingwei Ji, Zhenpei Yang, Nate Harada, Hao-tian Tang, Kan Chen, Charles R. Qi, Runzhou Ge, Kratarth Goel, Zoey Yang, Scott Ettinger, Rami Al-Rfou, Dragomir Anguelov, and Yin Zhou. Most: Multi-modality scene tokenization for motion prediction, 2024. 1
- [82] Kanthi Nagaraj, Dinesh Bharadia, Hongzi Mao, Sandeep Chinchali, Mohammad Alizadeh, and Sachin Katti. Numfabric: Fast and flexible bandwidth allocation in datacenters. In *Proceedings of the 2016 ACM SIGCOMM Conference*, page 188–201, New York, NY, USA, 2016. Association for Computing Machinery. 2
- [83] Arvind Narayanan, Xumiao Zhang, Ruiyang Zhu, Ahmad Hassan, Shuwei Jin, Xiao Zhu, Xiaoxuan Zhang, Denis Rybkin, Zhengxuan Yang, Zhuoqing Morley Mao, Feng Qian, and Zhi-Li Zhang. A variegated look at 5G in the wild: performance, power, and QoE implications. In *Proceedings of the 2021 ACM SIGCOMM 2021 Conference*, pages 610–625, New York, NY, USA, 2021. Association for Computing Machinery. 7
- [84] National Highway Traffic Safety Administration. NHTSA 2022 annual report safety recalls. Technical report, National Highway Traffic Safety Administration, 2023. 16
- [85] Nigamaa Nayakanti, Rami Al-Rfou, Aurick Zhou, Kratarth Goel, Khaled S Refaat, and Benjamin Sapp. Wayformer: Motion forecasting via simple & efficient attention networks. In *2023 IEEE International Conference on Robotics and Automation (ICRA)*, pages 2980–2987. IEEE, 2023. 2
- [86] Hieu Ngo, Hua Fang, and Honggang Wang. Cooperative perception with v2v communication for autonomous vehicles. *IEEE Transactions on Vehicular Technology*, 72(9): 11122–11131, 2023. 2
- [87] State of California Department of Motor Vehicles. Disengagement reports. <https://www.dmv.ca.gov/portal/vehicle-industry-services/autonomous-vehicles/disengagement-reports/>. 6, 15, 16
- [88] Published. ML scaling laws in autonomous driving - nuro - medium. <https://medium.com/nuro/at-nuro-we-conduct-an-ai-first-approach-by-using-ml-everywhere-5faf4657fff3>, 2024. Accessed: 2025-2-22. 1
- [89] Hang Qiu, Fawad Ahmad, Fan Bai, Marco Gruteser, and Ramesh Govindan. Avr: Augmented vehicular reality. In *Proceedings of the 16th Annual International Conference on Mobile Systems, Applications, and Services*, pages 81–95, 2018. 2
- [90] Moo-Ryong Ra, Anmol Sheth, Lily Mummert, Padmanabhan Pillai, David Wetherall, and Ramesh Govindan. Odessa: enabling interactive perception applications on mobile devices. In *Proceedings of the 9th international conference on Mobile systems, applications, and services*, pages 43–56, 2011. 2
- [91] Brian Tefft Rebecca Steinbach. American driving survey: 2022. Technical report, AAA Foundation for Traffic Safety, 2023. 15
- [92] Shaoqing Ren, Kaiming He, Ross Girshick, and Jian Sun. Faster R-CNN: Towards Real-Time Object Detection with Region Proposal Networks. In *Proceedings of the International Conferences on Advances in Neural Information Processing Systems (NeurIPS)*, pages 91–99, 2015. 5
- [93] Francisco Romero, Qian Li, Neeraja J Yadwadkar, and Christos Kozyrakis. Infaas: Automated model-less inference serving. In *USENIX Annual Technical Conference*, pages 397–411, 2021. 4, 15
- [94] J.S. Roy, Stuart A. Mitchell, Christophe-Marie Duquesne, Franco Peschiera, and Phillips Antony. Pulp. <https://github.com/coin-or/pulp>. Accessed 2024-9-14. 6
- [95] Peter Schafhalter, Sukrit Kalra, Le Xu, Joseph E Gonzalez, and Ion Stoica. Leveraging cloud computing to make autonomous vehicles safer. In *2023 IEEE/RSJ International Conference on Intelligent Robots and Systems (IROS)*, pages 5559–5566. IEEE, 2023. 1, 3
- [96] Gur-Eyal Sela, Ionel Gog, Justin Wong, Kumar Krishna Agrawal, Xiangxi Mo, Sukrit Kalra, Peter Schafhalter, Eric Leong, Xin Wang, Bharathan Balaji, Joseph E Gonzalez, and Ion Stoica. Context-aware streaming perception in dynamic environments. In *Proceedings of the European Conference on Computer Vision (ECCV)*, 2022. 2, 8
- [97] Jaime Sevilla, Lennart Heim, Anson Ho, Tamay Besiroglu, Marius Hobbhahn, and Pablo Villalobos. Compute trends across three eras of machine learning. In *2022 International Joint Conference on Neural Networks (IJCNN)*, pages 1–8. IEEE, 2022. 1, 2, 16
- [98] Shaoshuai Shi, Li Jiang, Dengxin Dai, and Bernt Schiele. Motion transformer with global intention localization and local movement refinement. *Advances in Neural Information Processing Systems*, 35:6531–6543, 2022. 2, 5
- [99] Shaoshuai Shi, Li Jiang, Dengxin Dai, and Bernt Schiele. Mtr++: Multi-agent motion prediction with symmetric scene modeling and guided intention querying. *IEEE Transactions on Pattern Analysis and Machine Intelligence*, 2024. 1
- [100] Anton Shilov. Nvidia’s h100 ai gpus cost up to four times more than amd’s competing mi300x — amd’s chips cost \$10 to \$15k apiece; nvidia’s h100 has peaked beyond \$40,000: Report. <https://www.tomshardware.com/tech-industry/artificial-intelligence/nvidias-h100-ai-gpus-cost-up-to-four-times-more-than-amds-competing-mi300x-amds-chips-cost-dollar10-to-dollar15k-apiece-nvidias-h100-has-peaked-beyond-dollar40000>, 2024. 15
- [101] Fei Sun, Fen Hou, Nan Cheng, Miao Wang, Haibo Zhou, Lin Gui, and Xuemin Shen. Cooperative task scheduling for

- computation offloading in vehicular cloud. *IEEE Transactions on Vehicular Technology*, 67(11):11049–11061, 2018. 2
- [102] Pei Sun, Henrik Kretzschmar, Xerxes Dotiwalla, Aurelien Chouard, Vijaysai Patnaik, Paul Tsui, James Guo, Yin Zhou, Yuning Chai, Benjamin Caine, Vijay Vasudevan, Wei Han, Jiquan Ngiam, Hang Zhao, Aleksei Timofeev, Scott Ettinger, Maxim Krivokon, Amy Gao, Aditya Joshi, Sheng Zhao, Shuyang Cheng, Yu Zhang, Jonathon Shlens, Zhifeng Chen, and Dragomir Anguelov. Scalability in perception for autonomous driving: Waymo open dataset. 2019. 2, 5, 7, 16
- [103] Yuxuan Sun, Xueying Guo, Sheng Zhou, Zhiyuan Jiang, Xin Liu, and Zhisheng Niu. Learning-based task offloading for vehicular cloud computing systems. In *2018 IEEE International Conference on Communications (ICC)*. IEEE, 2018. 2
- [104] Mingxing Tan, Ruoming Pang, and Quoc V. Le. EfficientDet: Scalable and Efficient Object Detection. In *Proceedings of the IEEE Conference on Computer Vision and Pattern Recognition (CVPR)*, 2020. 1, 2, 5
- [105] The Waymo Team. Waymo significantly outperforms comparable human benchmarks over 7+ million miles of rider-only driving. <https://waymo.com/blog/2023/12/waymo-significantly-outperforms-comparable-human-benchmarks-over-7-million/>, 2023. 6, 15
- [106] The Waymo Team. Fleet response: Lending a helpful hand to waymo’s autonomously driven vehicles. <https://waymo.com/blog/2024/05/fleet-response/>, 2024. 2, 16
- [107] Nicolo Valigi. Lessons Learned Building a Self-Driving Car on ROS. [https://roscon.ros.org/2018/presentations/ROSCon2018\\_LessonsLearnedSelfDriving.pdf](https://roscon.ros.org/2018/presentations/ROSCon2018_LessonsLearnedSelfDriving.pdf), 2018. 1, 7
- [108] Ashish Vaswani, Noam Shazeer, Niki Parmar, Jakob Uszkoreit, Llion Jones, Aidan N Gomez, Łukasz Kaiser, and Illia Polosukhin. Attention is all you need. In *Advances in Neural Information Processing Systems*. Curran Associates, Inc., 2017. 2
- [109] Nannan Wang, Xi Wang, Paparao Palacharla, and Tadashi Ikeuchi. Cooperative autonomous driving for traffic congestion avoidance through vehicle-to-vehicle communications. In *2017 IEEE Vehicular Networking Conference (VNC)*, pages 327–330. IEEE, 2017. 2
- [110] Wei-Hua Wang, Marimuthu Palaniswami, and Steven H. Low. Application-oriented flow control: fundamentals, algorithms and fairness. *IEEE/ACM Trans. Netw.*, 14(6): 1282–1291, 2006. 2
- [111] Waymo. Waymo Safety Report: On the Road to Fully Self-Driving. <https://storage.googleapis.com/sdc-prod/v1/safety-report/SafetyReport2018.pdf>. 15
- [112] Ross Wightman. efficientdet-pytorch. <https://github.com/rwightman/efficientdet-pytorch>. Accessed: 2024-9-6. 5
- [113] Benjamin Wolfe, Bobbie Seppelt, Bruce Mehler, Bryan Reimer, and Ruth Rosenholtz. Rapid holistic perception and evasion of road hazards. *Journal of experimental psychology: general*, 149(3):490, 2020. 1, 2
- [114] Xiaoyang Wu, Li Jiang, Peng-Shuai Wang, Zhijian Liu, Xihui Liu, Yu Qiao, Wanli Ouyang, Tong He, and Hengshuang Zhao. Point transformer v3: Simpler, faster, stronger. *arXiv preprint arXiv:2312.10035*, 2023. 1
- [115] Dongzhu Xu, Anfu Zhou, Xinyu Zhang, Guixian Wang, Xi Liu, Congkai An, Yiming Shi, Liang Liu, and Huadong Ma. Understanding operational 5g: A first measurement study on its coverage, performance and energy consumption. In *Proceedings of the Annual conference of the ACM Special Interest Group on Data Communication on the applications, technologies, architectures, and protocols for computer communication*, pages 479–494, 2020. 8, 17
- [116] Ran Xu, Jayoung Lee, Pengcheng Wang, Saurabh Bagchi, Yin Li, and Somali Chaterji. Liteconfig: Cost and content aware reconfiguration of video object detection systems for mobile gpus. In *Proceedings of the Seventeenth European Conference on Computer Systems*, pages 334–351, 2022. 2
- [117] Ran Xu, Fangzhou Mu, Jayoung Lee, Preeti Mukherjee, Somali Chaterji, Saurabh Bagchi, and Yin Li. Smartadapt: Multi-branch object detection framework for videos on mobiles. In *Proceedings of the IEEE/CVF Conference on Computer Vision and Pattern Recognition*, pages 2528–2538, 2022. 2
- [118] Fisher Yu, Haofeng Chen, Xin Wang, Wenqi Xian, Yingying Chen, Fangchen Liu, Vashisht Madhavan, and Trevor Darrell. Bdd100k: A diverse driving dataset for heterogeneous multitask learning. In *Proceedings of the IEEE/CVF conference on computer vision and pattern recognition*, pages 2636–2645, 2020. 5
- [119] Chaoqun Yue, Ruofan Jin, Kyoungwon Suh, Yanyuan Qin, Bing Wang, and Wei Wei. LinkForecast: Cellular link bandwidth prediction in LTE networks. *IEEE Trans. Mob. Comput.*, 17(7):1582–1594, 2018. 8
- [120] Jiang-Tian Zhai, Ze Feng, Jihao Du, Yongqiang Mao, Jiang-Jiang Liu, Zichang Tan, Yifu Zhang, Xiaoqing Ye, and Jingdong Wang. Rethinking the open-loop evaluation of end-to-end autonomous driving in nuscenes. *arXiv preprint arXiv:2305.10430*, 2023. 8
- [121] Xiaohua Zhai, Alexander Kolesnikov, Neil Houlsby, and Lucas Beyer. Scaling vision transformers. In *Proceedings of the IEEE/CVF Conference on Computer Vision and Pattern Recognition*, pages 12104–12113, 2022. 1, 2
- [122] Haoyu Zhang, Ganesh Ananthanarayanan, Peter Bodik, Matthai Philipose, Paramvir Bahl, and Michael J Freedman. Live Video Analytics at Scale with Approximation and Delay-Tolerance. In *Proceedings of the 14<sup>th</sup> USENIX Conference on Networked Systems Design and Implementation (NSDI)*, 2017. 2
- [123] Menghan Zhang, Xianliang Jiang, Guang Jin, Penghui Li, and Haiming Chen. CapRadar: Real-time adaptive bandwidth prediction for dynamic wireless networks. *Comput. Netw.*, 233(109865):109865, 2023. 8
- [124] Shigeng Zhang, Yinggang Li, Xuan Liu, Song Guo, Weiping Wang, Jianxin Wang, Bo Ding, and Di Wu. Towards real-

time cooperative deep inference over the cloud and edge end devices. *Proceedings of the ACM on Interactive, Mobile, Wearable and Ubiquitous Technologies*, 4(2):1–24, 2020. [2](#)

- [125] Xumiao Zhang, Anlan Zhang, Jiachen Sun, Xiao Zhu, Y Ethan Guo, Feng Qian, and Z Morley Mao. Emp: Edge-assisted multi-vehicle perception. In *Proceedings of the 27th Annual International Conference on Mobile Computing and Networking*, pages 545–558, 2021. [2](#)

## A. Appendix

### A.1. Economic Feasibility

In this section, we analyze whether our approach is feasible when taking into account the cost of network transmission (Appendix A.1.1) and compute (Appendix A.1.2).

#### A.1.1. Network Cost

Commercial cellular network usage is charged primarily by the GB [52]. We conduct an analysis of consumer-marketed cellular data plans reported in the Cable.co.uk global mobile data pricing dataset [53]. Tab. 2 shows the cheapest consumer-facing (*i.e.* SIM card) cost per GB of data in a selection of countries, along with the computed cost per hour of streaming an average of 100 Mbps of data continuously. We note that we expect wholesale pricing, especially geofenced to a particular region, to be considerably cheaper.

We see that prices vary widely from as low as \$0.001/GB in Israel, to \$0.75/GB in the US, up to over \$2 in Norway. This wide range in pricing requires careful consideration in deployment: in countries such as Israel, the price of cellular data transmission running our method is trivial at \$0.04 per hour of driving, assuming an average utilization of 100 Mbps. In some other countries, including the U.S. with a price of \$33.76 per hour, prices are considerably higher and present an economic obstacle at present to using remote resources. However, we note that at or below the 10th percentile of global prices – which includes major markets such as India, Italy, and China – mobile networks are cost-effective at \$2.78 per hour of driving. We expect much of the rest of the world to follow to these prices, as median price per GB has continuously decreased 4× over the years our dataset covers, 2019-2024, from \$5.25 to \$1.28.

In the short-term, in countries with high cellular data prices, operators may choose to reduce costs by selectively utilizing remote resources to aid in high-stress driving environments *e.g.* during poor visibility due to weather and busy urban areas. Alternatively, it would be feasible for AV fleet operators to deploy their own dedicated locale-specific wireless network at cheaper cost.

#### A.1.2. Compute Cost

Cloud providers offer competitive access to GPUs: Lambda Labs hourly pricing ranges from \$0.80 for an NVIDIA A6000 GPU to \$2.49 for an NVIDIA H100 GPU [8].

Cloud compute offers a number of additional valuable advantages not available on the car. Cloud access allows operators to configure which compute resources to use based on compute requirements and cost sensitivity. Remote resources cannot be stolen or damaged in an accident. AV fleet operators can take advantage of statistical multiplexing to share a smaller set of compute for their fleet (Appendix A.2). Furthermore, model serving systems can optimize resource

Rank	Country	\$/GB	\$/Hour
1	Singapore	\$0.07	\$3.30
2	Netherlands	\$0.36	\$16.08
3	Norway	\$2.09	\$94.14
4	United States	\$0.75	\$33.76
5	Finland	\$0.26	\$11.62
–	China	\$0.27	\$12.28
–	Israel	\$0.001	\$0.04
–	10th pct	\$0.062	\$2.78
–	Median	\$0.37	\$16.84

Table 2: Network costs ranked highest by AV readiness score [63]. We include China as a major AV market [35], Israel as the cheapest cellular market, and the 10th percentile and median global country by network price. Hourly rates assume an average constant network utilization of 100 Mbps.

utilization by batching and scheduling requests [32, 50, 93], resulting in further price improvements.

**Total cost.** We estimate total hourly cost of remote resources at \$5.27, with \$2.78 from the network (at the 10th global percentile) and \$2.49 from compute for an H100. We emphasize that the true cost of cloud compute is likely lower due to better efficiency when operating at scale.

### A.2. Cloud Compute Multiplexing

Sharing upgraded compute costs across a fleet of vehicles presents a significant opportunity to further reduce costs over upgrading on-vehicle compute due to statistical multiplexing of cloud resources. Though cars still need to retain their own GPUs, shared upgrades to cloud resources can instantly benefit fleets of AVs. The average driver in the U.S. drives only 60.2 minutes per day [91], *i.e.* a vehicle utilization of 4.2%. This under-utilization is more pronounced for personal vehicles than autonomous ride-hailing services, which we estimate to be ~59% based on the ratio of peak to average hourly Uber rides in New York City [43]. Considering this under-utilization, the cost of purchasing a single H100 GPU (~\$40k [100]) is equivalent to renting an H100 in the cloud for an 44 years for the average American driver, and 3 years for the average autonomous ride-hailing vehicle.

### A.3. Further Discussion

**Practical Necessity of TURBO.** We acknowledge that there are limited deployments of commercial AVs today [3, 12, 17] which outperform humans on safety benchmarks [13, 111], and we rely on this capability to provide a fallback when network connectivity is unavailable. However, “safety” as both a concept and a metric is continuous, measured as a rate of incident occurrence [13, 87, 111], and AVs must merely exceed human-level safety for deployment [105]. TURBO seeks to improve safety beyond what on-car systems can provide today and presents an opt-in solution for AV providers

to improve the accuracy of their services by leverage cloud and network infrastructure.

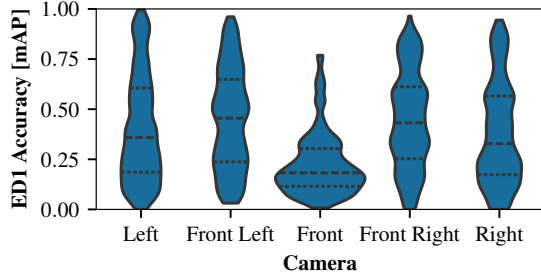


Figure 9: Accuracy distribution when evaluating *EfficientDet-D1* on each frame for each camera. The accuracy distributions vary by camera angles due to differences in content, e.g. frequency, distance, and types of objects. Dashed lines are the median, dotted are 25th and 75th percentile.

For AVs with different sets of economic and technical requirements (e.g. operating in low-stakes environments and with little compute, such as autonomous delivery robots [7, 14, 46]), TURBO may provide a viable method of improving existing or expanding functionality such as safe high-speed operation or decreasing the rate of human intervention [106].

As AVs deployments expand, we expect to see more outdated AV models with older generations of hardware on the road<sup>7</sup>. As SOTA compute hardware capabilities, and correspondingly SOTA model sizes and requirements, continue to rapidly increase [36, 78, 97], outdated hardware will prevent older vehicles from taking advantage of the latest model advancements. While upgrades to on-vehicle compute hardware are possible, they may be difficult and expensive to roll out in practice. As a reference, fix rates for recalls are only 52-64% [84] despite being free, mandatory upgrades that mitigate critical safety risks (e.g. faulty brake systems [16]). TURBO provides access to SOTA cloud hardware, enabling older AVs to use highly accurate, SOTA models.

Finally, SOTA hardware requires increasingly stringent operating environments, ranging from high power and cooling needs for GPUs [71], to strong intolerance to movement or temperature changes for quantum computing [9]. As a result, the only way to integrate methods that require such hardware is via the network, and TURBO presents a system that can manage this integration. Hence, we firmly believe that such a system is useful today and will become more applicable to the real world as current technical and economic trends continue.

**Limitations.** Our design does not consider scheduling the order of messages, *i.e.* delaying transmission for one service to make more bandwidth available to another service to reduce its transmission time. Likewise, we do not consider

<sup>7</sup>The average lightweight vehicle age in the U.S. is 12.5 years [24].

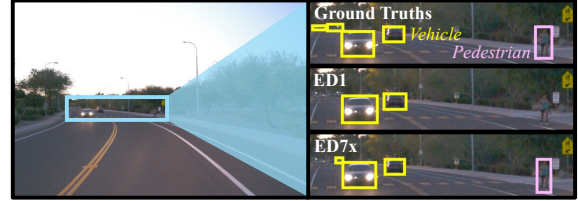


Figure 10: *More accurate detectors provide a better understanding of the surroundings.* In this scene from the Waymo Open Dataset [102], *EfficientDet-D1* (ED1 – center) detects the two nearby vehicles but misses the pedestrian on the side of the road, resulting a mean average precision (mAP) of 25%. In contrast, highly accurate *ED7x* model (bottom) detects the pedestrian and both nearby vehicles, but generates an incorrect bounding box for one of the distant vehicles, resulting in an mAP of 75%.

executing consecutive tasks in the cloud without returning back to the car which could further reduce data transmission. In this work, we develop an approach to offloading parallelizable tasks and leave scheduling extensions (e.g. exploiting task dependencies to decrease the amount of data transmitted on the network) to future work.

TURBO relies on 5G coverage for fast network bandwidths and low round-trip times. While 5G coverage is rapidly expanding, it is not ubiquitous [15].

Finally, TURBO requires the AV operator to configure  $f_s$  (Sec. 3.3) to ensure that the ILP maximizes the end-to-end performance of the AV system, as maximizing average accuracy across all services may not necessarily translate to maximal *safety*. We cannot provide this directly for the operator as each operator’s particular AV pipeline design may differ. However, we believe that configurations of  $f_s$  may be automatically discoverable using simulations and machine learning; we leave this area to future work.

**Implications for AV design.** Our results suggest that using cloud resources to run more accurate models can significantly improve accuracy, enabling AVs to make better-informed, high quality decisions which benefit safety. Beyond safety events, cloud models can reduce the frequency of remote interventions [106] by improving the AV’s understanding of its surroundings. Reducing interventions improves the experience for riders, reduces the cost of operating AVs, and is a key metric used by government officials to assess AV system safety [87].

At the same time, we note that adopting the cloud raises new concerns; the cellular connection is elevated to a more important role, which increases the need for security in the AV system as well as improvements to the performance, reliability, and availability of the cellular connection.

**Implications for Mobile Network Stakeholders.** If AVs integrate cloud computing, the demand for cellular network resources will increase massively. In 2022, 283 million vehicles were registered in the United States [18] alone out of



an estimated 1.5 billion vehicles in use worldwide [38]. If only a fraction of these vehicles use the cloud to enhance autonomous capabilities, mobile networks must support millions of new users with long-running, data-intensive streaming workloads. Moreover, AVs demand better up-link bandwidth and lower round-trip latencies. Prior work reports that a major contributor to cellular RTT latency is the “backhaul” portion of the network, connecting the radio base station to the cellular core [115]. Consequently, cellular network operators will need to prioritize backhaul latency improvements and potentially provide network guarantees for AVs and other safety-critical connected systems.

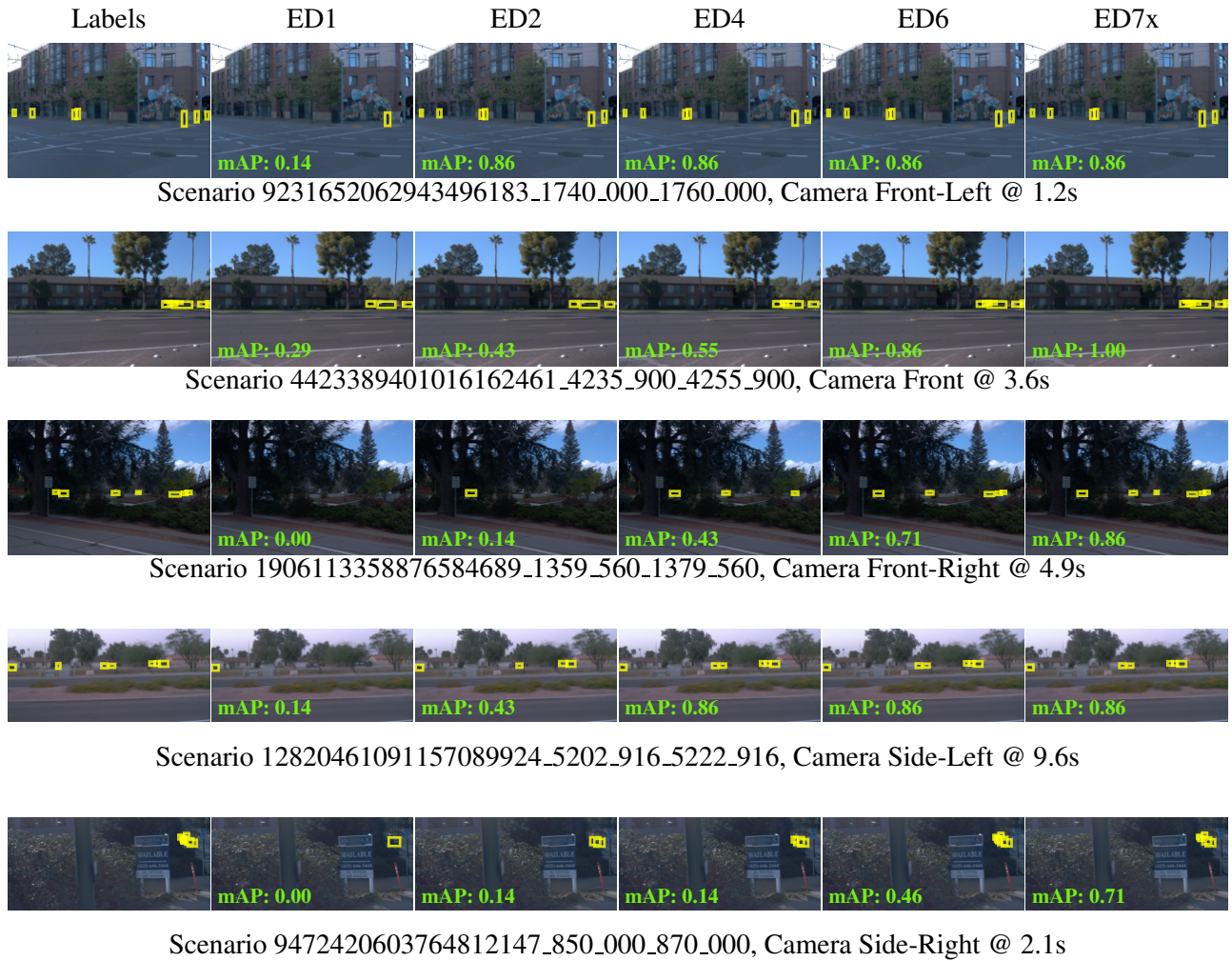


Figure 11: *Qualitative differences in object detectors.* We visualize the bounding box predictions of various *EfficientDet (ED)* object detection models fine-tuned on the Waymo Open Dataset, and find that larger models can better detect distant and small objects.